Chemical Engineering Journal 166 (2011) 738–743

Contents lists available at ScienceDirect

Chemical Engineering Journal

journal homepage: www.elsevier.com/locate/cej

Hydrogen production by methane decomposition and catalytic partial oxidation of methane over $Pt/Ce_xGd_{1-x}O_2$ and $Pt/Ce_xZr_{1-x}O_2$

Maria D. Salazar-Villalpando[a,*], Adam C. Miller[b]

[a] US Department of Energy, National Energy Technology Laboratory, 3610 Collins Ferry Rd, Morgantown, WV 26507, USA
[b] Chemical Engineering Department, West Virginia University, Morgantown, WV 26506, USA

ARTICLE INFO

Article history:
Received 10 August 2010
Received in revised form 3 November 2010
Accepted 19 November 2010

Keywords:
Partial oxidation of methane
Zirconia doped ceria
Hydrogen production
Methane decomposition
Gadolinium doped ceria

ABSTRACT

Hydrogen production by methane decomposition and catalytic partial oxidation of methane (CPOM) over $Pt/(Ce_{0.91}Gd_{0.09})O_{2-x}$ and $Pt/(Ce_{0.56}Zr_{0.44})O_{2-x}$ were studied. Results show that during the methane decomposition tests, in the absence of gaseous oxygen, hydrogen and CO were the main products and very small quantities of CO_2 were recorded. The generation of these products lasted for about 2 h, indicating that in the catalytic stability of these materials, the carrier plays an important factor. The addition of Gd and Zr cations to ceria had a positive effect on the catalysts stability. Regarding the catalytic partial oxidation of methane, a stable hydrogen production was recorded for 20 h. Here, it is proposed that the formation of a Pt–O–Ce bond causes high stability of Pt in Ce-containing supports under oxidizing conditions at high temperatures because this bond may act as an anchor, inhibiting the sintering of Pt. The deposited carbon during the catalytic tests was oxidized and the CO_2 profiles showed a sharper peak appearing at a lower temperature and a broader peak at the higher temperature. The first peak may correspond to the oxidation of coke on and in the vicinity of the metal and the second CO_2 peak may represent the coke on the carrier. The CPOM as a function of O/C ratio was studied. It was observed that the catalyst with a higher ionic conductivity, $Pt/(Ce_{0.91}Gd_{0.09})O_{2-x}$, generated a lower amount of deposited carbon.

Published by Elsevier B.V.

1. Introduction

Direct utilization of methane eliminates the need for pre-reformers and greatly reduces the complexity, size, and cost of the overall SOFC systems. However, due to severe carbon deposition caused by the cracking of methane, the conventional Ni-based anodes are generally considered inappropriate for the direct utilization of hydrocarbons. Ni–YSZ cermets are used as the anode material almost exclusively in SOFC. However, when Ni catalysts are tested with hydrocarbon feed stocks, they are prone to deactivation through the formation of carbonaceous deposits on the catalyst surface. There is presently much interest in using methane feeds in SOFCs directly, thus avoiding the endothermic steam reforming stage. Development of economically feasible electrochemical reactors requires, however, to achieve high currents and low electrode polarization; this may be only possible using catalytically active anode components containing ceria and Pt [1]. Solid oxide electrolytes based on ceria doped oxides are considered to be one of the most promising candidate materials for use in single-chamber intermediate temperature solid oxide fuel cells, because they offer a considerably higher ionic conductivity than YSZ in the range of 450–800 °C. The substitution of Ce^{4+} by suitable trivalent cations such as Gd^{3+}, Sm^{3+}, Y^{3+} or La^{3+} has been carried out in ceria-based electrolytes because they enhance the chemical stability, increase the ionic conductivity and suppress the reducibility of ceria-based materials. The most effective substitutes seem to be Gd_2O_3 and Sm_2O_3, possibly due to the fact that they minimize the changes in lattice parameter [2].

The thermodynamics of methane reforming reactions demand elevated temperatures (~1073 K or above) to obtain a high methane conversion and, under these conditions, metal agglomeration is favored, leading to a decrease in activity with time on stream. At high temperatures, the decomposition of methane occurs through successive steps of dissociation of CH_4, producing C^* species ($CH_4 \rightarrow C^* + 2H_2$) and the disproportionation of CO at low temperatures ($2CO \rightarrow C^* + CO_2$). Under low oxygen/carbon ratio conditions, required in the CPOM processes to obtain a H_2/CO ratio around 2, the reaction rates can be un-equilibrated and decrease carbon removal ($C^* + O^* \leftrightarrow CO^* + *$), which can result in carbon accumulation on the metal surface [3]. Catalyst deactivation in the partial oxidation of methane is often attributed to coking of the active sites via concurrent carbon deposition [4]. As a result, overall reactor operation—which admits coke minimization and/or catalyst regeneration—has been a strategic objective. These two processes,

* Corresponding author. Tel.: +1 304 2855 427.
E-mail address: maria.salazar@netl.doe.gov (M.D. Salazar-Villalpando).

1385-8947/$ – see front matter. Published by Elsevier B.V.
doi:10.1016/j.cej.2010.11.076

however, require reliable and adequate information on the structural characteristics and removal kinetics of the carbon residue. Ceria, a stable fluorite-type oxide, has been studied for various reactions utilizing its redox properties, which can be further enhanced in the presence of a metal or metal oxide. Otsuka et al. [5,6] have showed that ceria is able to directly convert methane to syngas with $H_2/CO = 2$ at temperatures higher than 600 °C. Ceria has also been examined as a promoter of both the activity and selectivity of supported Ni or Pt catalysts for the partial oxidation of methane [7,8,33,34]. Ceria-supported Ni with high Ni-loading (13 wt.%) was reported by Tang et al. [9] to be an active catalyst for the POM at temperatures above 750 °C. However, this catalyst rapidly deactivates due to carbon deposition. Thus, the substitution of Ni by Pt and the use of doped ceria carriers seem to be a practical approach to mitigate carbon formation and reach stable performances.

The objective of this work was to study the catalytic behavior of Pt/gadolinium-doped ceria and Pt/zirconia-doped ceria during the catalytic decomposition of methane and the catalytic partial oxidation of methane.

2. Experimental

2.1. Catalyst synthesis

The mixed oxides $(Ce_{0.56}Zr_{0.44})O_{2-x}$ (ZDC50) and $(Ce_{0.91}Gd_{0.09})O_{2-x}$ (GDC10) were prepared by co-precipitation of the precursors followed by hydrothermal crystallization. Then, they were calcined at 800 °C for 4 h to stabilize the surface area and ball milled to reduce particle size. The catalysts Pt(1 wt.%)/ZDC50 and Pt(1 wt.%)/GDC10 were prepared using a modified incipient wetness technique. Following, it was granulated within a particle size range of 150–500 μm and then calcined at 500 °C for 1 h in flowing air. The ionic conductivities as a function of temperature, surface areas, XRD and temperature programmed profiles of these materials have been published somewhere else [8].

2.2. Catalytic performance

In order to examine methane decomposition over Pt/ZDC50 or Pt/GDC10, a sample of 100 mg was loaded into the sample chamber of an Autochem 2910 system, and the test was carried out using a CH_4(5 vol.%)–He mixture with a flow rate of 25 ml/min at standard temperature and pressure (STP). The instrument measured the CH_4 uptake by the catalyst while heating the sample at a rate of 10 °C/min; the experimental data was recorded at 1-s intervals from ambient temperature to 760 °C. A mass spectrometer was connected online to analyze the feed and product gas streams. A cold trap at the outlet of the reactor condensed any water out of the latter stream. Regarding the stability tests for the CPOM reaction, experiments were carried out in a tubular reactor (i.d. = 8 mm) with a time on stream of 24 h. In order to determine if low oxygen concentrations would cause catalysts instability, tests were performed at oxygen/carbon ratio (O/C) = 0.4. A ceramic furnace heated the reactor and controlled the temperature with a thermocouple centered within the catalyst bed. To analyze the feed and product gas streams, an on line mass spectrometer was connected to the reactor. The CPOM reaction experiments were carried out setting the reactor temperature at 700 °C and a gas hourly space velocity (GHSV) = 146,000 h^{-1}. In another set of experiments, the effect of O/C ratio on the partial oxidation of methane of Pt-doped ceria catalysts was studied varying O/C ratio over the range of 0.4–1. The experiments were initiated by bringing the reactor to 700 °C, while purging with N_2. Once the temperature was achieved, the corresponding reacting mixture was delivered to the reactor and the experiment started. Several mixtures of CH_4, air and N_2 were delivered to the reactor in order to meet these requirements. The methane flow rate was constant and air and N_2 flows were adjusted to meet the O/C ratio required in every test. In order to determine the amount of carbon generated during the methane decomposition and the CPOM tests, a mixture of air and N_2 was delivered to the reactor and CO_2 concentration was monitored by the on-line mass spectrometer. The carbon oxidation was allowed to continue until less than 0.05 vol% of CO_2 was detected. In order to study the effect of the redox processes over the catalysts, five consecutive tests were carried out to study the CPOM at a constant O/C = 0.66, following the same experimental conditions in every experiment.

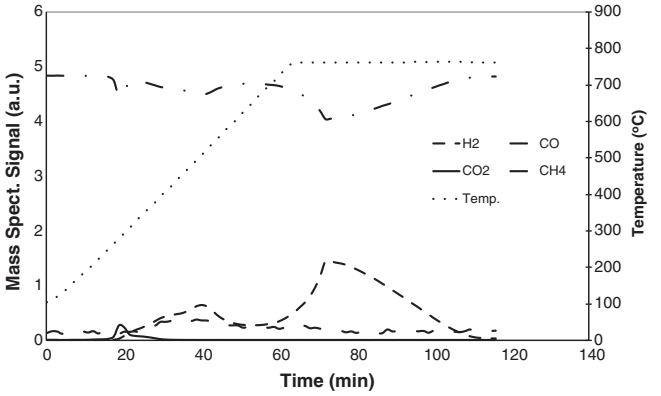

Fig. 1. Product distribution of the methane decomposition reaction over Pt/ZDC50.

3. Results

3.1. Methane decomposition

Fig. 1 shows the product distribution as a function of temperature and time on stream for the decomposition of methane over Pt/ZDC50 obtained by temperature-programmed experiments. Only methane was delivered to the reactor, without gaseous oxygen. The direct oxidation of methane starts around 680 °C and the maximum rate of conversion does not occur until the temperature reaches 750 °C, as it can be observed by the signal of the mass spectrometer for methane. Hydrogen production lasted for about 2 h. It has been explained [10] that in the stability of supported catalysts, the carrier plays an important factor. The addition of promoters to ceria, especially rare earth oxides, results in more stable catalysts. Thus, it seems that in our work, the addition of Gd and Zr cations to ceria had a positive effect on the catalysts stability. The carriers GDC10 and ZDC50 contribute to metal dispersion making the catalyst more resistant to poisoning by coke and to the sintering process. In addition, these materials participate to the reaction mechanism as oxygen storage components. Hydrogen production during this catalytic process has been suggested to form through the following reaction mechanism [11]:

(1) Methane adsorption and dissociation on the active sites

$$(CH_4)_g \rightarrow (CH_3)_{ads} + (H)_{ads}$$

(2) Progressive dissociation releasing hydrogen-rich adsorbed

$$(CH_3)_{ads} \rightarrow (CH_2)_{ads} + (H)_{ads}$$

$$(CH_2)_{ads} \rightarrow (CH)_{ads} + (H)_{ads}$$

(3) Crystallization and growth of the carbon deposits

$$(CH)_{ads} \rightarrow (C)_{ads} + (H)_{ads}$$

$$(C)_{ads} + 1/n(Cn)_c$$

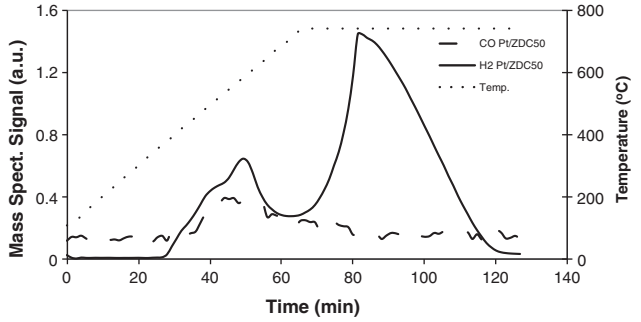

Fig. 2. H_2 and CO mass spectrometer signals during the methane decomposition reaction on Pt/ZDC50.

(4) Formation and desorption of H_2 gas

$$(H)_{ads} + (H_2)_g$$

Figs. 2 and 3 show the mass spectrometer signal for CO and H_2 for Pt/ZDC50 and Pt/GDC10, respectively, during the methane decomposition reaction. The concentration of H_2 was much higher than CO with both materials. Otsuka et al. [5,6] have demonstrated that the reaction of methane with ceria in the absence of gaseous oxygen selectively produced a synthesis gas with a H_2/CO ratio of 2, while CO_2 and H_2O were formed as the main products in the presence of gaseous oxygen. Therefore, the use of an oxygen storage component as oxidant in the absence of gas-phase oxygen could be a promising approach to the direct partial oxidation of methane. It has also been noted that the decomposition of methane may lead to CO formation via reaction of the carbonaceous residue with the oxygen of the oxide support [12]. Thus, here it is proposed that CO and CO_2 may have formed through CH_x species with the oxygen from the catalyst, according to the following reactions [13]

$$CH_x + O \rightarrow CHO + (x-1)H$$

The decomposition of CHO will lead to CO formation

$$CHO \rightarrow CO + H$$

And further reaction of CHO will form CO_2

$$CHO + O \rightarrow CO_2 + H$$

Here, it is proposed that the surface and lattice oxygen of Pt/GDC10 and Pt/ZDC50 are able to participate in catalytic reactions in the absence of gaseous oxygen. It is known that doped ceria carriers, specifically ceria has stable oxidation states (Ce^{3+}/Ce^{4+}) and mediates the amount of available oxygen in the catalytic reactions, releasing oxygen under reducing conditions and taking up oxygen under oxidizing conditions [14]. It has been reported that the formation of hydrogen and CO was enhanced by the incorporation of

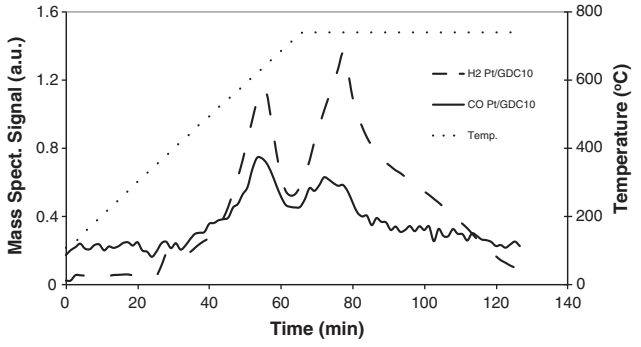

Fig. 3. H_2 and CO mass spectrometer signals during the methane decomposition reaction on Pt/GDC10.

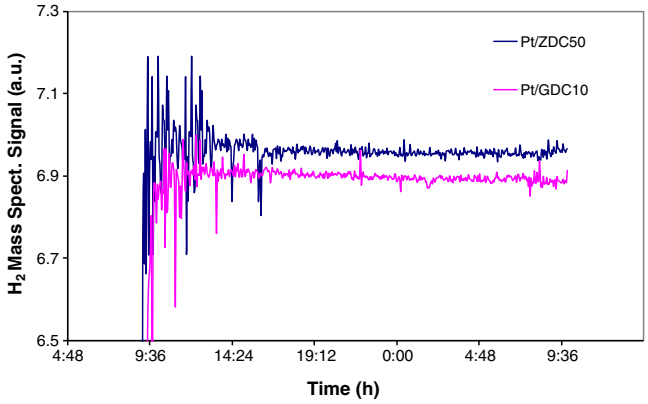

Fig. 4. Stability tests of the catalytic partial oxidation of methane.

zirconia into ceria up to a ZrO_2 20% content. Further increase in the content of ZrO_2, decreased the rates of H_2 and CO formation [15]. The results obtained here showed that the main products are H_2 and CO during the reaction of methane over Pt/GDC10 and Pt/ZDC50 in the absence of gaseous oxygen, which may lead to the conclusion that the characteristics of these materials would allow its use in the anodes of SOFCs for the direct electrochemical oxidation of methane. Higher CO concentration was observed over Pt/GDC10 than over Pt/ZDC50. It has been proposed that the substitution of Ce with Gd, Eu and Sm, whose ionic radii are close to the critical radius value of CeO_2 causes neither expansion nor contraction of fluorite lattice structure of ceria [16] and enhances oxygen ionic conductivity. It has been reported a higher ionic conductivity value for Pt/GDC10 than for Pt/ZDC50 [8], which may explain the higher CO concentration over Pt/GDC10.

3.2. Catalyst stability for CPOM reaction

One of the main issues in the catalytic production of H_2 is the development of stable catalysts. Hence, the stability of Pt/GDC10 and Pt/ZDC50 for the production of hydrogen during the CPOM was evaluated as a function of time on stream. The CPOM was carried out in the presence of oxygen, at O/C molar ratio = 0.4, keeping the reactor temperature at 700 °C. Results of these stability tests are shown in Fig. 4. Both catalysts showed similar hydrogen production, a slightly higher concentration was observed over Pt/ZDC50 with respect to Pt/GDC10. Stable performance was observed for about 20 h. In our results, the higher activity of Pt/ZDC50 than Pt/GDC10 may be due to the higher thermal activity of Pt/ZDC50. It has been proposed that the formation of a Pt–O–Ce bond causes high stability of Pt in Ce-containing supports under oxidizing conditions at high temperature because this bond may act as an anchor, inhibiting the sintering of Pt [10]. The stability of Pt/GDC10 and Pt/ZDC50 may also be due to the redox properties of ceria. It has been explained that cerium oxide has a very high oxygen exchange capacity [14]. This capacity is associated with the ability of cerium to act as an oxygen buffer through the storage/release of O_2 due to the Ce^{4+}/Ce^{3+} redox couple. The enhancement of the reducibility of CeO_2 and doped-ceria has been observed after redox treatments at high temperatures [17]. It has been observed that parameters such as Pt dispersion, composition of the support, composition of the reactant and reaction temperature can affect the stability and activity of catalysts in reactions of methane reforming [10]. In addition, it has been suggested that carriers containing ceria have the property to anchor metallic Pt which helps to maintain the surface area and avoids the migration and coalescence of Pt crystallites. During the CPOM, Pt is reduced by CH_4, decreasing the PtO_2 content in the catalyst. Thus, Pt is predominantly in a reduced state, which

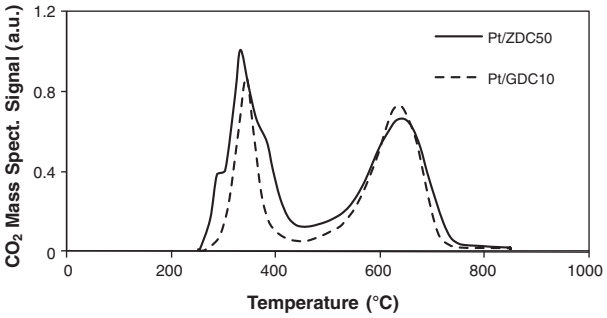

Fig. 5. Temperature programmed oxidation of deposited carbon.

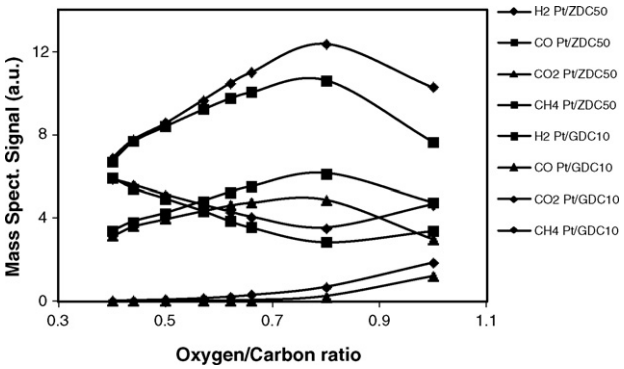

Fig. 6. Product distribution for the catalytic partial oxidation of methane.

suppresses sintering via the formation of mobile and volatile PtO_2. Moreover, it has been proposed that carbon deposition is one of the factors that cause catalyst deactivation [18]. Thus, in the stability tests with Pt/GDC10 and Pt/ZDC50, it is reasonable to assume that there is equilibrium between the rates of activation of CH_4 and of carbon removing.

3.3. Carbon deposition during the stability tests

The carbon generated on the catalysts during the stability tests over the Pt/GDC10 and Pt/ZDC50 was oxidized by temperature programmed oxidation and the CO_2 was recorded by a mass spectrometer connected on line, results are shown in Fig. 5. In general, a higher amount of CO_2 was recorder for Pt/ZDC50 than Pt/GDC10. Two peaks were observed for both catalysts tested. The first peak appeared in the temperature range, 250–430 °C, and the second peak appeared in the temperature range 520–715 °C. Similar results have been published [19], a sharper peak appearing at a lower temperature and a broader peak at the higher temperature. It has been proposed that the first peak corresponds to the oxidation of coke on and in the vicinity of the metal. The second CO_2 peak may represent the coke on the carrier. Moreover, it has been suggested that only a small part of the coke is located on the metal, while a larger part is placed close to the metal and on the carrier. It has been explained that coke initially blocks the metallic sites, but as it grows, the carbonaceous material is deposited on carrier. Two different combustion kinetics rates have been calculated for the coke that is located at the two positions [20]. In our tests with Pt/GDC10 and Pt/ZDC50, particularly, it seems that a higher carbon oxidation rate was observed for the peak recorder at lower temperatures (250–430 °C). The oxidation rate of the carbon that presumably was deposited on the carrier seemed to show a lower oxidation rate, this peak appeared at high temperatures (520–715 °C).

3.4. Partial oxidation of methane as a function of O/C ratio

Fig. 6 shows the product distribution during the CPOM as a function of O/C ratio. At O/C = 1, the mass spectrometer signal of H_2 and CO is lower than at O/C = 0.8. It has been suggested that the CPOM depends on the catalyst temperature, which in turn is a function of O/C. The CPOM generates high yields of H_2 and CO at high catalyst temperatures (i.e., at high O/C). Optimal values have been reached around O/C = 1.2 [21]. Here, we observed optimal catalytic performance at O/C = 0.8, which may be due to the effect of redox cycles that the catalyst undergo. Enhanced catalytic performance during the CPOM has been observed under redox cycles [8]. In our work, catalytic tests as a function of redox treatments were performed at constant O/C = 0.66. Figs. 7 and 8 show hydrogen production over Pt/GDC10 and Pt/ZDC50 as a function of redox cycles, respectively. Higher H_2 production was observed as the number of redox cycle was increased. Thus, these results in Figs. 7 and 8

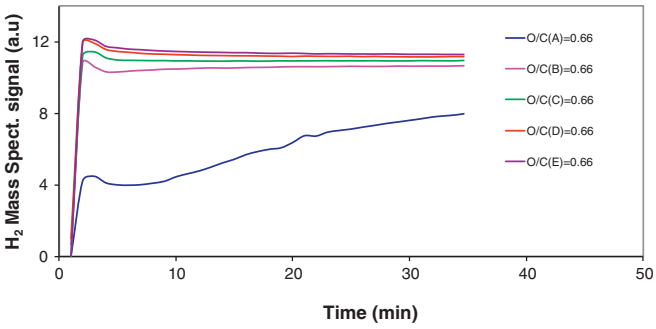

Fig. 7. Redox treatments during the CPOM over Pt/GDC10 at 700 °C at constant O/C = 0.66.

may explain results in Fig. 6, a higher catalytic performance was observed at O/C = 0.8 than O/C = 1 because the catalytic activity was enhanced by redox treatments. Further results of the CPOM at different O/C ratios in Fig. 6 illustrated that decreasing the O/C ratio in the feed caused the decrease of hydrogen and CO production. At lower O/C, the CH_4 conversion dropped because O_2 is the stoichiometrically limiting component. The reaction mechanism of the CPOM is a combination of the partial oxidation and steam reforming [22]. It has been proposed [21] that the reaction mechanism of the CPOM at lower O/C ratios than the stoichiometric remains the same as at O/C = 1, only the ratio of H_2/CO production varied. In our results, a slightly higher H_2 and CO production were observed over Pt/ZDC50 than over Pt/GDC10 during the CPOM as a function of O/C. The higher catalytic activity of the former catalyst than Pt/GDC10 could be caused by the higher catalyst stability of Pt/ZDC50 than Pt/GDC10. It is known that one of the major drawbacks of ceria is its poor resistance towards sintering [23]. Ceria has a cubic related structure and sinters equally along the three *x*, *y*, and *z* axis. One of

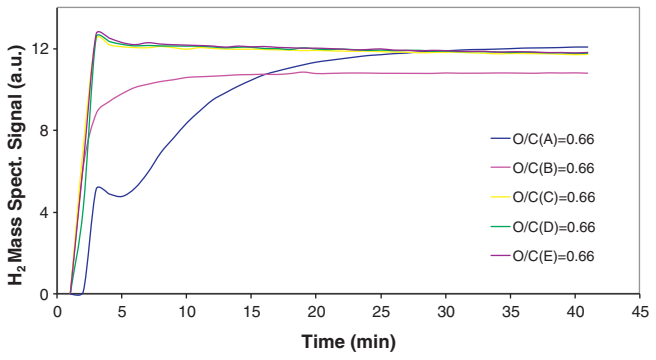

Fig. 8. Redox treatments during the CPOM over Pt/ZDC50 at 700 °C at constant O/C = 0.66.

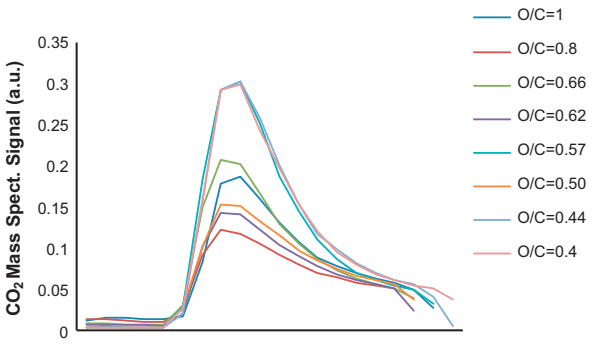

Fig. 9. Temperature programmed oxidation of deposited carbon over Pt/GDC10.

the main breakthroughs has been the use of zirconia as a dopant. The metal oxide ZrO_2 is a refractory oxide having the same fluorite structure as ceria. Despite slightly different ionic radii, i.e., 0.97 Å (Ce^{4+}) and 0.84 Å (Zr^{4+}), zirconium anions can be introduced in ceria lattice without too much stress. Solid solutions of ceria and zirconia are more thermally stable than pure ceria. These oxides are more resistance to sintering and have shown high oxygen storage capacity. The addition of zirconia to ceria generates oxygen vacancies in the solid and then provides a way of minimizing the stress generated in the ceria lattice by adopting the unfavorable eight-fold coordination [24]. It has also been found that the creation of oxygen vacancies can also improve the mobility of oxygen in the bulk, increasing the efficiency of CeO_2 as oxygen storage material. Moreover, it has been observed that in addition to the stabilization of the cubic phase, the use of dopants may favour both phase and surface area [25]. It has also been observed that the addition of zirconium into the CeO_2 lattice greatly improves the oxygen storage capacity. An optimum has been observed for $Ce_xZr_{(1-x)}O_2$ oxides with x between 0.6 and 0.8. These oxides have a fluorite-type structure, which appears to be an important parameter. The largest OSC was obtained for $Ce_{0.63}Zr_{0.37}O_2$ with 219 μmol/g, which OSC calculated to be four times larger than the OSC of pure ceria [26]. It has been suggested that in the case of CeO_2, the storage of oxygen at 400 °C is restricted to the surface. On the opposite, in the case of $Ce_{0.63}Zr_{0.37}$, oxygen storage takes place not only at the surface but also in the bulk [27].

The carbon generated on the catalysts during the CPOM, varying the O/C ratio, over the Pt/GDC10 and Pt/ZDC50 was oxidized at 850 °C and the CO_2 generated was recorded by a mass spectrometer connected on line, Figs. 9 and 10. As illustrated by the mass spectrometer signals, it appears that a lower carbon deposition was observed over Pt/GDC10 than over Pt/ZDC50. These results may be due to the higher ionic conductivity of Pt/GDC10 than Pt/ZDC50 [7]. According to Steele [28], the highest ionic single crystal (bulk grain) conductivity of the doped ceria is exhibited by the $Ce_{0.8}Gd_{0.2}O_{1.9}$. Based on a number of studies [31,32], it has been suggested that the most important parameter for oxide ion conductivity in fluorites is the cation match with the critical radius. This means that the highest ionic conductivity is obtained when the radius of the dopant is as close to the critical radius of ceria as possible. Doped ceria has shown higher ionic conductivity than ceria. The oxygen ion conductivity mechanism is the hopping of oxide ions to vacant sites. The total ionic conductivity may be separated in bulk and grain boundary. Even in very pure materials, the intrinsic limit of the grain boundaries remains 100–1000 times lower than the bulk material. It was also found that very small grains might affect the bulk conductivity adversely because the dopant is extracted to the grain boundaries to an extent that the grains become practically undoped [29]. In materials with grain sizes of a micron and above the grain boundary phase constitutes a very tiny fraction of the material, and therefore the total ionic conductivity is not necessarily significantly affected. Moreover, it has been suggested that oxygen diffusion coefficients are predicted to be larger in bulk ceria than in nanocrystalline CeO_2, and precious metal doping suppresses the formation of grain boundaries when the smaller dopant cation is more easily accommodated than large Ce(III) ions in the partially reduced structure [30]. In our results, lower carbon deposition was observed over Pt/GDC10 than over Pt/ZDC50. These results may be due to the higher ionic conductivity of Pt/GDC10 than Pt/ZDC50. The high catalytic activity and high resistance to carbon deposition may be caused by the higher capacity of the Pt–O–Ce bond, which acts as an anchor, to transfer O* from the carrier to Pt atoms [10], resulting in carbon oxidation and an improved accessibility of CH_4 to the active sites, mitigating carbon deposition. Thus, ionic conductivity of Pt/GDC10 than Pt/ZDC50 played a major role in the amount of deposited carbon.

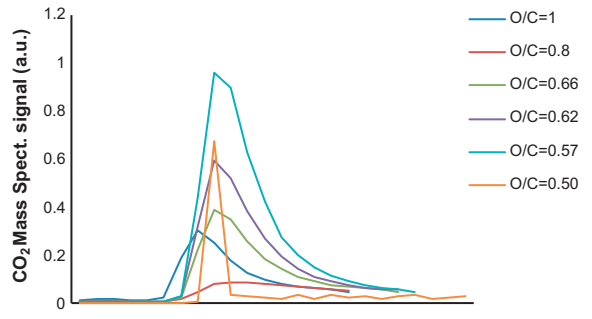

Fig. 10. Temperature programmed oxidation of deposited carbon over Pt/ZDC50.

4. Conclusions

By studying the catalytic methane decomposition reaction and the CPOM over $Pt/(Ce_{0.91}Gd_{0.09})O_{2-x}$ and $Pt/(Ce_{0.56}Zr_{0.44})O_{2-x}$, it is proposed that their characteristics would allow its use in SOFCs for the direct electrochemical oxidation of methane. Regarding the CPOM reaction, a stable production of syn-gas was recorded for 20 h. Here, it is suggested that the formation of a Pt–O–Ce bond causes high stability of Pt in Ce-containing supports under oxidizing conditions at high temperature because this bond may act as an anchor, inhibiting the sintering of Pt. During the oxidation of deposited carbon, the CO_2 profiles showed a sharper peak appearing at a lower temperature and a broader peak at the higher temperature. The first peak may correspond to the oxidation of coke on and in the vicinity of the metal and the second CO_2 peak may represent the coke on the carrier. The CPOM as a function of O/C ratio was also studied, and it was observed that the catalyst with a higher ionic conductivity, $Pt/(Ce_{0.91}Gd_{0.09})O_{2-x}$ generated a lower amount of deposited carbon.

Acknowledgment

Miller would like to thank the ORISE program at NETL, Morgantown, WV.

References

[1] R.J. Gorte, H. Kim, J.M. Vohs, J. Power Sources 106 (2002) 10.
[2] M. Morales, S. Pinol, M. Segarra, J. Power Sources 194 (2009) 961.
[3] J. Wei, E. Iglesia, J. Phys. Chem. B 108 (2004) 4094.
[4] C.H. Bartholomew, Appl. Catal. A: Gen. 212 (2001) 17.
[5] K. Otsuka, Y. Wang, E. Sudana, I. Yamanaka, J. Catal. 175 (1998) 152.
[6] K. Otsuka, T. Ushiyam, I. Yamanaka, Chem. Lett. (1993) 1517.
[7] M.D. Salazar-Villalpando, B. Reyes, Int. J. Hydrogen Energy 34 (2009) 9723.
[8] M. Salazar, D.A. Berry, T.H. Gardner, D. Shekhawat, D. Floyd, Appl. Catal. A: Gen. 310 (2006) 54.
[9] S. Tang, J. Lin, K.L. Tan, Catal. Lett. 51 (1998) 169.

[10] P. Ferreira-Aparicio, A. Guerrero-Ruiz, I. Rodriguez-Ramos, Appl. Catal. A: Gen. 170 (1998) 177.
[11] D.P. Serrano, J.A. Botas, J.L.G. Fierro, R. Guil-Lopez, P. Pizarro, G. Gomez, Fuel 89 (2010) 1241.
[12] R. Ryoo, S.H. Joo, S. Jun, T. Tsubakiyama, O. Terasaki, Stud. Surf. Sci. Catal. 135 (2001) 150.
[13] J.H. Bitter, K. Seshan, J.A. Lercher, J. Catal. 176 (1998) 93.
[14] H.C. Yao, Y.F. Yu Yao, J. Catal. 86 (1984) 254.
[15] P.K.K. Pantu, G.R. Gavals, Appl. Catal. A: Gen. 193 (2000) 203.
[16] P. Fornasiero, R. Di Monte, G. Ranga Rao, J. Kaspar, V. Sergo, G. Gubitosa, A. Ferrero, M. Griziani, J. Catal. 164 (1996) 173.
[17] F. Fally, V. Perrichon, H. Vidal, J. Kaspar, G. Blanco, J.M. Pintado, S. Bernal, G. Colon, Catal. 59 (2000) 373.
[18] T. Zhu, M. Flytzani-Stephanopoulos, Appl. Catal. A 208 (2001) 403.
[19] K.M. Hardimana, C.G. Coopera, A.A. Adesina, R. Lange, Chem. Eng. Sci. 61 (2006) 2565.
[20] I. Sierra, J.E. Andreĭ s, T. Aguayo, J.M. Arandes, J. Bilbao, Appl. Catal. B: Environ. 94 (2010) 108.
[21] R. Horn, K.A. Williams, N.J. Degenstein, A. Bitsch-Larsen, D. Dalle Nogare, S.A. Tupy, L.D. Schmidt Horn, J. Catal. 249 (2007) 380.
[22] O. Deutschmann, L.D. Schmidt, AIChE J. 44 (1998) 2465.
[23] J. Kaspar, P. Fornasiero, M. Graziani, Catal. Today 50 (1999) 285.
[24] P. Li, I.W. Chen, J.E. Penner-Hahn, J. Am. Soc. 77 (1994) 118.
[25] P. Vidmar, P. Fornasiero, J. Kapar, G. Gubitosa, M. Graziani, J. Catal. 171 (1997) 160.
[26] Y. Madier, C. Descorme, A.M. Le Govic, D. Duprez, J. Phys. Chem. B 103 (1999) 10999.
[27] A. Trovarelli, F. Zamar, J. Llorca, C. de Leiternburg, G. Dolcetti, J.T. Kiss, J. Catal. 169 (1997) 490.
[28] B.C.H. Steele, Solid State Ionics 129 (2000) 95.
[29] D. Yu, A.S. Nowick, J. Solid State Chem. 35 (1980) 325.
[30] T.X.T. Sayle, S.C. Parker, D.C. Sayle, Faraday Discuss. 134 (2007) 377.
[31] J. Kilner, Solid State Ionics 8 (1983) 201.
[32] J. Kilner, R.J. Brook, Solid state Ionics 6 (1982) 237.
[33] M.D. Salazar-Villalpando, A. Berry David, A. Cugini, Int. J. Hydrogen Energy 35 (2010) 1998.
[34] M.D. Salazar-Villalpando, D.A. Berry, T.H. Gardner, Int. J. Hydrogen Energy 332 (2008) 695.